Rheol. Acta **20**, 163 – 178 (1981)

ISSN 0035-4511 / ASTM-Coden: RHEAAK

Department of Chemical Engineering, Massachusetts Institute of Technology, Cambridge, Massachusetts

Shear flow properties of concentrated solutions of linear and star branched polystyrenes

K. Yasuda, R. C. Armstrong, and *R. E. Cohen*

With 17 figures and 4 tables

(Received August 28, 1980)

Summary

The linear viscoelastic and viscometric functions have been determined for solutions of well-characterized monodisperse linear and star-branched polystyrenes and for commercial, polydisperse polystyrene. The value of the product $c\bar{M}_w$ for these solutions was large and was obtained by using both high and low $\bar{M}_w$.

The effect of structure on the rheological properties was determined by examining how parameters in a modified Carreau viscosity equation (used to fit the data) varied with c, $\bar{M}_w$, and branching. No enhancement effects on the rheological properties were observed because of branching.

The Cox-Merz rule was observed to describe the similarities between the viscosity and complex viscosity for most of the monodisperse samples studied. The broad molecular weight distribution polystyrene solutions did not follow this empiricism.

Zusammenfassung

Für Lösungen wohldefinierter monodisperser linearer und sternförmiger Polystyrole sowie kommerzieller polydisperser Polystyrole werden sowohl die linear-viskoelastischen als auch die viskosimetrischen Funktionen bestimmt. Der Wert des Produkts $c\bar{M}_w$ für diese Lösungen ist groß, er wird gleicherweise für Proben mit niedrigem und hohem $\bar{M}_w$ erhalten.

Der Einfluß der Struktur auf die rheologischen Eigenschaften ist in der Weise erfaßt, daß die Variation der Parameter der zur Anpassung der Meßwerte verwendeten modifizierten Viskositätsgleichung nach Carreau mit c, $\bar{M}_w$ und dem Verzweigungsgrad untersucht wird. Es werden keine Verstärkungswirkungen bei den rheologischen Eigenschaften infolge der Verzweigungen beobachtet.

Es wird gefunden, daß die Cox-Merz-Regel die Ähnlichkeit zwischen stationärer und komplexer Viskosität bei den meisten untersuchten monodispersen Proben gut wiedergibt. Dagegen gehorchen die Polystyrollösungen mit breiter Molgewichtsverteilung dieser empirischen Gleichung nicht.

Key words

Viscometric function, viscoelastic function, polystyrene solution

1. Introduction

In this paper we present results on the rheological properties of well-characterized polystyrene solutions in shearing flows. The structural parameters that we have varied include concentration, molecular weight, molecular weight distribution, and branching. We have characterized the frequency-dependent behavior of these materials in small-amplitude oscillatory shearing flow by means of the customary complex viscosity $\eta^* = \eta' - i\eta''$ (or complex modulus $G^* = G' + iG'' = i\omega\eta^*$). The nonlinear shearing behavior is given by the viscosity η and first normal-stress coefficient Ψ_1 determined in steady shear flow. It is a significant part of this study that we have measured in each of these flows the viscous or dissipative property (η', η) and also the "elastic" or energy storage property (η'', Ψ_1).

There are several motives for undertaking this study. First it is of intrinsic interest to understand the influence of molecular architecture and solution concentration on both linear viscoelastic and large amplitude steady shearing properties. Secondly, availability of both the linear and non-linear properties on the same well-characterized samples would provide a useful tool in evaluating constitutive equations. Thirdly, there have long been known to exist striking similarities in the shapes of η' and η, and to a lesser extent η'' and $\frac{1}{2}\dot{\gamma}\Psi_1$. Prior to this study, quantitative evaluation of this pair of "analogies" has been frustrated by lack of data on all four properties for the same materials. One of our objectives has thus been to evaluate the predictive success of these analogies and to determine the effect of structure on this success.

There have been numerous previous studies of the linear viscoelastic and steady shear behavior of undiluted polymers and polymer solutions. It is not possible from these results to draw the kinds of structure-property inferences that we seek. For example, many of those studies report either linear viscoelastic or viscometric (steady shear flow) properties alone (1, 2, 3). Among those studies containing both linear viscoelastic and viscometric properties, many do not have both Ψ_1 and G' data (4, 5). Also high shear rate data on η and Ψ_1 are scarce (2, 6) and sometimes questionable.

Commercial polymers with broad molecular weight distributions have been characterized rheologically in the molten state. However, we are not aware of published data on these materials which contain both viscometric and linear viscoelastic properties. For this reason we have included commercial, undiluted polystyrene in our experimental program.

For constructing structure-property relationships it is preferable to use narrow molecular weight distribution polystyrene. Because of the small quantities of polymer available, it is most practical to study these in solution and to infer melt behavior from these results. Several studies (5, 7 – 9) have presented both linear viscoelastic and viscometric properties of moderately concentrated, well characterized polystyrene solutions. In these studies the product of concentration c and molecular weight $\bar{M}_w$ has been chosen to be approximately the same as for commercial polystyrene solutions and melts. These large values of $c\bar{M}_w$ were obtained with $\bar{M}_w$ ($8.6 \cdot 10^5 - 5.5 \cdot 10^6$) higher than for commerical polystyrene (10^5) and concentrations that are low (0.07 – 0.22 g/ml). The experimental motivation for this choice of c and $\bar{M}_w$ is that in cone and plate rheometry, steady shear flow measurements at fixed, large $c\bar{M}_w$ are possible to higher shear rates with low c and high $\bar{M}_w$ as compared to high c and low $\bar{M}_w$. We think that this is a significant limitation of the earlier studies, since there is no guarantee that the rheological behavior should be a function only of the product $c\bar{M}_w$ for concentrated solutions and melts.

In the present study we have used a wide range of molecular weights and large concentrations to examine rheological behavior over a wide range of c and $\bar{M}_w$. To circumvent the high shear rate instabilities in cone and plate flow inherent in this range of c and $\bar{M}_w$ we have used a capillary viscometer. This allowed us to cover the same wide shear rate range as in other studies (2, 6) with large c and low $\bar{M}_w$.

We have also examined the effects of long chain branching on both linear viscoelastic and viscometric properties; anionically polymerized, star-branched polysytrenes have been used as models to study long chain branching. It has been found that in dilute solutions, properties of star-branched polymers can be correlated to those of linear polymers by correcting for size shrinkage due to branching; this is done by means of the ratio g of the radius of gyration of the branched polymer to that of the linear polymer (10)

$$g \equiv \frac{\langle s^2 \rangle_{\text{branched}}}{\langle s^2 \rangle_{\text{linear}}}. \qquad [1]$$

For star polymers with f branches each of the same molecular weight it has been shown that (11)

$$g \equiv \frac{3f - 2}{f^2}. \qquad [2]$$

Concentrated solutions and melts of star-branched polymers have been observed to show "enhancement" effects (12), that is, abnormally high steady shear flow properties as compared to their linear counterparts, even after molecular size has been corrected with g. In particular the zero-shear-rate viscosity η_0 of branched polymers is found to increase more rapidly than $\bar{M}_w^{3.4}$ as is observed for linear polymers. Of particular interest in this study is the effect of branching on similarities between linear viscoelastic and viscometric properties. No data are available in the literature for assessing the impact of branching on these similarities although several studies have been published on either the viscometric (2, 6, 12, 13) or linear viscoelastic (3, 14, 15, 16) properties of star-shaped polystyrene, polybutadiene, hydrogenated polybutadiene, and polyisoprene.

2. Experimental materials and methods

2.1. Materials

The three groups of samples used in this study were: (1) linear, narrow molecular weight distribution polystyrenes (Pressure Chemical Co.), (2) star-branched polystyrenes with narrow molecular weight distribution (Dr. P. Rempp, CNRS, Strasbourg), and (3) commercial polystyrene with broad molecular weight distribution (Dow Chemical Co., Styron). These are listed in table 1 along with pertinent structural information. Table 2 lists the solutions prepared from these samples that were used in this study. In table 2 we have also listed some linear polystyrene solutions studied by Ashare (17) which we include in our data analysis. More detail on these samples and solution prepara-

Table 1. Polystyrene sample characteristics

	$\bar{M}_w$	$\bar{M}_w/\bar{M}_n$	f	$(\bar{M}_w)_b$	g	$g\bar{M}_w$	g_2	$[\eta]^{35}_{1\text{-CN}}$
Linear[1])								ml/g
	$2 \cdot 10^6$	1.30	2					440
	$3.9 \cdot 10^5$	1.10	2					125
	$1.1 \cdot 10^5$	1.06	2					50
	$3.7 \cdot 10^4$	1.06	2					22
	$1.75 \cdot 10^4$	1.06	2					16
Commercial: Styron[2])	$3.69 \cdot 10^5$	3.45	2					
Star branched[3])	$7.9 \cdot 10^5$	1.25	8	$1.05 \cdot 10^5$	0.344	$2.72 \cdot 10^5$	0.219	98
	$6.05 \cdot 10^5$	1.18	7	$8.80 \cdot 10^4$	0.388	$2.35 \cdot 10^5$	0.252	88
	$2.06 \cdot 10^5$	1.05	6.4	$3.2 \cdot 10^4$	0.420	$8.65 \cdot 10^4$	0.219	41
	$1.25 \cdot 10^5$	1.12	8	$1.56 \cdot 10^4$	0.344	$4.30 \cdot 10^4$	0.277	24

f = number of arms
$(\bar{M}_w)_b$ = Molecular weight of each arm
g = size correction factor for radius of gyration (eq. [1])
g_2 = size correction factor for steady state compliance (eq. [21])
$[\eta]^{35}_{1\text{-CN}}$ = intrinsic viscosity at 35 °C in 1-chloronaphthalene
[1]) Pressure Chemical Co.
[2]) Dow Chemical Co.
[3]) Dr. P. Rempp of CNRS, Strasbourg

tion and testing methods are given by Yasuda (18).

2.2. Methods

The linear viscoelastic properties were measured in the eccentric rotating disk mode of the Rheometrics Mechanical Spectrometer. As a check on these results we also tested several of the samples in the forced-oscillation cone-and-plate mode on the same instrument.

The steady shear flow measurements were performed primarily with the cone-and-plate mode of the Mechanical Spectrometer. In order to check the low shear rate limits we obtained with these data and the time-temperature superposition principle, we also used an Instron Rotary Rheometer (Model 3250) with a sensitive transducer to measure directly the zero-shear-rate values in the cone-and-plate mode. In order to make high shear-rate measurements of viscosity to test our use of time-temperature superposition we used a capillary rheometer (Instron Model 3211) with special capillaries (L/D = 125 and 212). Details of these instruments and the relative advantages and disadvantages of each can be found elsewhere (18).

As mentioned above, in order to extend the effective frequency or shear rate range of a given instrument, we have used the principle of time-temperature superposition (10). Measurements were thus made on the Mechanical Spectrometer at temperatures ranging from −5 °C to 40 °C. At each temperature as large a variation as possible in shear rate or frequency was covered.

3. Results

Figure 1 presents typical steady shear flow data obtained on the Mechanical Spectrometer in the cone-and-plate mode. The expected shear-rate dependence of the viscosity, η, is clearly revealed over the range of shear rates covered as well as the strong dependence of the zero-shear-rate viscosity on temperature. The shear-rate and temperature dependence of the primary normal-stress coefficient, Ψ_1, are also apparent, although the low shear rate limiting values $\Psi_{1,0}$ are not as clearly defined as the corresponding zero-shear-rate viscosities η_0.

For all of the solutions studied (see table 2) we found that it was possible to describe the temperature dependence of the nonlinear viscometric functions by a system of reduced variables similar to that commonly employed for linear viscoelastic data (cf. 10, Ch. 11). For

Table 2. Samples used in rheological measurements

Sample identification	$g\bar{M}_w$ (g/mole)	c (g/ml)	$gc\bar{M}_w$ (g²/mole · ml)	$c[\eta_0]$ (−)	Solvent[4])	Symbol used in figures
Linear polystyrene solutions:						
A1	$2 \cdot 10^6$	0.30	$6.0 \cdot 10^5$	132	1-CN	
A2	$2 \cdot 10^6$	0.15	$3.0 \cdot 10^5$	66	1-CN	
A3	$2 \cdot 10^6$	0.088	$1.76 \cdot 10^5$	34.7	1-CN	
B1	$3.9 \cdot 10^5$	0.45	$1.76 \cdot 10^5$	56.3	1-CN	
B2	$3.9 \cdot 10^5$	0.30	$1.17 \cdot 10^5$	37.5	1-CN	
B3	$3.9 \cdot 10^5$	0.344	$1.34 \cdot 10^5$	43	DMP	
C1	$1.1 \cdot 10^5$	0.52	$5.72 \cdot 10^4$	26	1-CN	
C2	$1.1 \cdot 10^5$	0.45	$4.95 \cdot 10^4$	22.5	1-CN	
C3	$1.1 \cdot 10^5$	0.344	$3.78 \cdot 10^4$	17.2	1-CN	
D1	$3.7 \cdot 10^4$	0.62	$2.29 \cdot 10^4$	13.6	1-CN	
D2	$3.7 \cdot 10^4$	0.45	$1.67 \cdot 10^4$	9.9	1-CN	
D3	$3.7 \cdot 10^4$	0.344	$1.27 \cdot 10^4$	7.6	DMP	
E1	$1.75 \cdot 10^4$	0.62	$1.09 \cdot 10^4$	9.9	1-CN	
E2	$1.75 \cdot 10^4$	0.45	$7.88 \cdot 10^3$	7.2	1-CN	
Samples from ref. 15	$1.8 \cdot 10^6$					
	$8.6 \cdot 10^5$					
	$4.11 \cdot 10^5$					
Star branched polystyrene solutions:						
F1	$2.72 \cdot 10^5$	0.45	$1.22 \cdot 10^5$	44.0	1-CN	
F2	$2.72 \cdot 10^5$	0.30	$8.6 \cdot 10^4$	26.3	1-CN	
G1	$2.35 \cdot 10^5$	0.45	$1.06 \cdot 10^5$	39.4	1-CN	
H1	$8.65 \cdot 10^4$	0.45	$3.89 \cdot 10^4$	18.5	1-CN	
J1	$4.30 \cdot 10^4$	0.45	$1.94 \cdot 10^4$	10.9	1-CN	
Styron						
K1	$3.69 \cdot 10^5$	0.473	$1.75 \cdot 10^5$		1-CN	
K2	$3.69 \cdot 10^5$	0.420	$1.55 \cdot 10^5$		1-CN	
K3	$3.69 \cdot 10^5$	0.368	$1.36 \cdot 10^5$		1-CN	
K4	$3.69 \cdot 10^5$	0.315	$1.16 \cdot 10^5$		1-CN	
K5	$3.69 \cdot 10^5$	0.368	$1.36 \cdot 10^5$		DMP	
K6	$3.69 \cdot 10^5$	0.263	$9.71 \cdot 10^4$		DMP	
K7	$3.69 \cdot 10^5$	0.315	$1.16 \cdot 10^5$		DBP	
K8	$3.69 \cdot 10^5$	0.315	$1.16 \cdot 10^5$		KMC-A	

[4]) Solvent designation: 1-CN = 1-Chloronaphthalene; KMC-A = Alkylnaphthalene (mixture); DBP = Dibutylphthalate; DMP = Dimethylphthalate

each sample, logarithms of the values of zero-shear-rate-viscosity, $\log \eta_0$, obtained in each of several isothermal experiments (generally 5 or more) were plotted against $1/T$, and excellent straight-line fits were obtained in all cases. The apparent activation energies ΔH, defined by:

$$\frac{\eta_0(T)}{\eta_0(T_0)} = e^{-\frac{\Delta H}{R}\left(\frac{1}{T}-\frac{1}{T_0}\right)} \qquad [3]$$

were determined from the slopes of these plots and are presented in figure 2 as a function of sample concentration; there is a clear trend of increasing activation energy with increasing concentration, and no systematic effect of molecular weight or molecular structure is seen. Shift factors, a_T, for time-temperature superposition, were calculated from the activation energies by:

$$a_T = \frac{T_0}{T} e^{-\frac{\Delta H}{R}\left(\frac{1}{T}-\frac{1}{T_0}\right)} = \frac{T_0}{T}\frac{\eta_0(T)}{\eta_0(T_0)} \qquad [4]$$

and were applied to the isothermal measurements to compute reduced viscometric functions as follows:

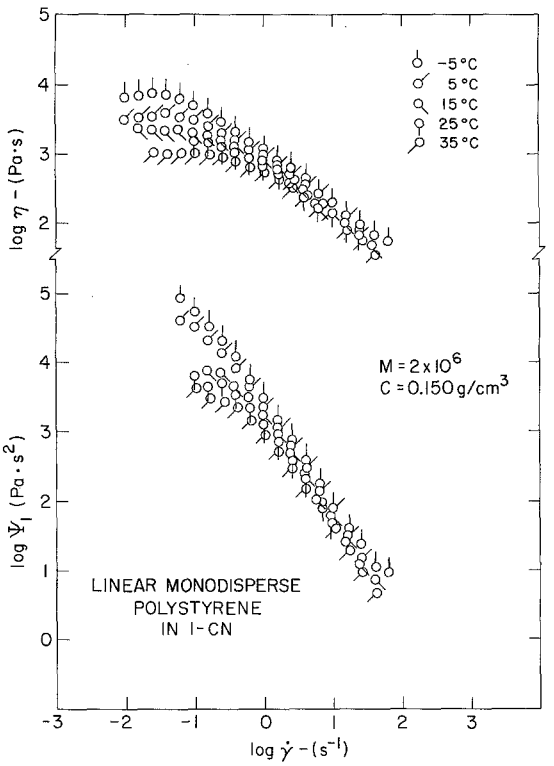

Fig. 1. Viscosity and primary normal-stress coefficient as functions of shear rate at five temperatures

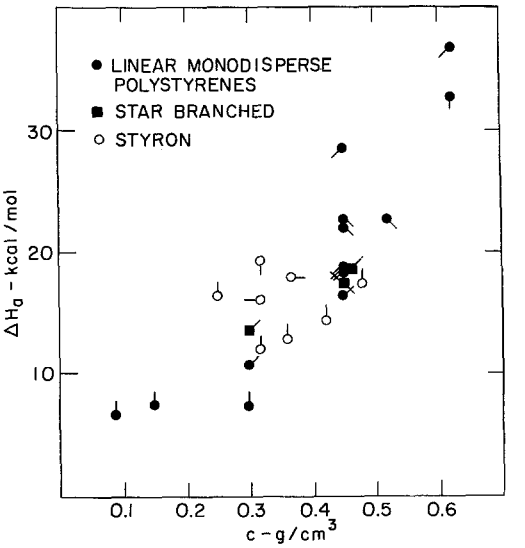

Fig. 2. Activation energy for flow as given by the temperature dependence of the zero-shear-rate viscosity (eq. [3]). Symbols are defined in table 2

$$\eta_r(\dot{\gamma}_r) = \eta \cdot \frac{\eta_0(T_0)}{\eta_0(T)} = \eta \cdot \frac{T_0}{a_T T}, \qquad [5]$$

$$\Psi_{1,r}(\dot{\gamma}_r) = \Psi_1 \cdot \frac{T_0}{a_T^2 T} \qquad [6]$$

$$\dot{\gamma}_r = a_T \dot{\gamma}. \qquad [7]$$

The appearance of the (T_0/T) factor in eq. [6] arises from assuming that all components of stress are reduced in the same manner as the shear stress.

The success of the method is indicated in figure 3 where "master curves" are shown for the viscosity and primary normal-stress difference ($N_1 = \Psi_1 \dot{\gamma}^2$). The reference temperature T_0 on this plot (and all subsequent plots) is 25 °C, and thus the master curves represent the expected isothermal behavior at this temperature. In this figure and in subsequent figures and discussion we will delete the subscript "r" on the reduced rheological functions. As can be seen in this figure, only about one decade in shear rate is gained by using temperature reduc-

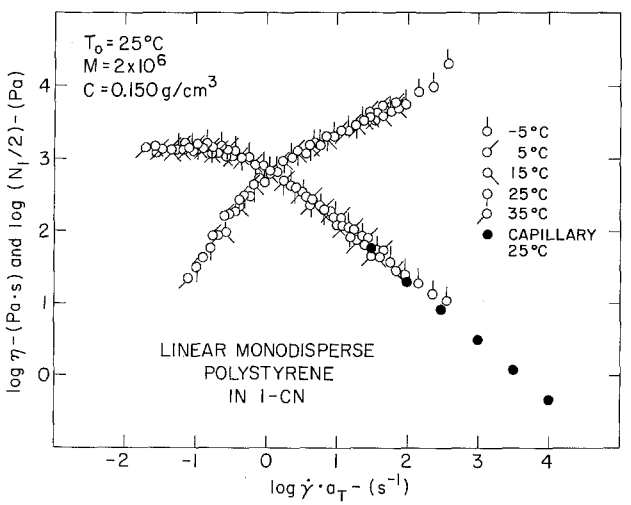

Fig. 3. Master curves for viscosity and primary normal-stress difference at 25 °C obtained by time-temperature superposition of the results in figure 1. High shear rate data taken in a capillary viscometer (●) at 25 °C were not shifted

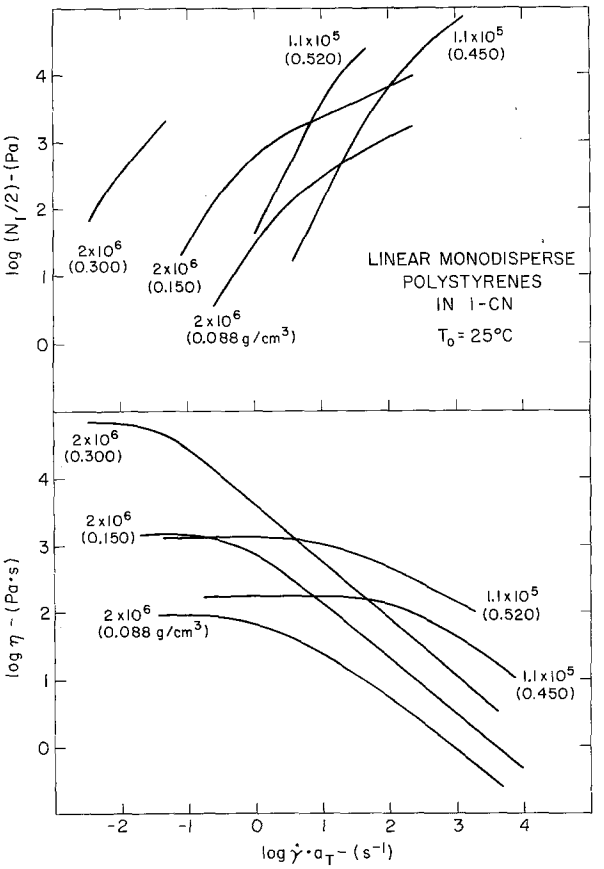

Fig. 4. Master curves for viscosity and the primary normal-stress difference at 25 °C for typical linear, monodisperse polystyrene/1-CN solutions examined in this study. The molecular weight for each sample is given beside the respective curve; the concenttration is in parentheses

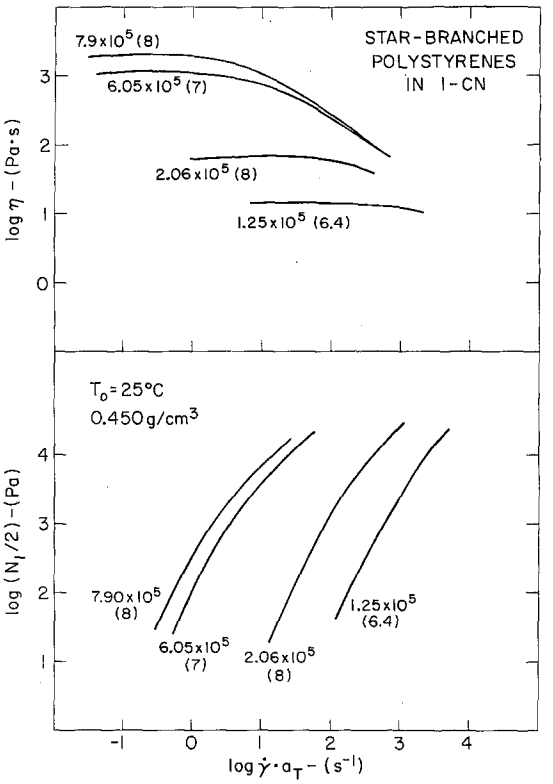

Fig. 5. Master curves for viscosity and the primary normal-stress difference at 25 °C for typical star-branched, monodisperse polystyrenes in 1-CN. All solutions have concentration 0.45 g/cm^3. The molecular weight is given beside each curve along with the number of arms in the star (in parentheses)

tion over the range −5 °C to 40°C. Viscosities at higher shear rates were measured at 25 °C in a capillary viscometer, and these data are shown in figure 3 as filled circles. The agreement between the capillary data and cone-and-plate data in the overlapping shear rate region is typical of all samples tested.

Figures 4−6 show various selected master curves which represent the typical trends shown by the steady shear flow data obtained in this investigation. In figure 4 the effect of concentration on the viscosity and the primary normal-stress difference is shown for two narrow distribution linear polystyrenes of differing molecular weights. Note that the viscosity master curves cover a much wider range of shear rates than those for N_1 owing to the availability of capillary data at high shear rates for this material function and to large experimental uncertainty in the normal-stress measurements at very low shear rates. Figure 5 presents some of the η and N_1 master curves obtained for the star-branched polystyrenes. In this figure all curves represent data obtained at a fixed concentration of 0.450 g/cm^3; differences in the material behavior shown here reflect differences in molecular weight and degree of branching in the various polystyrene samples. Figure 6 shows the steady shear behavior of various solutions of the broad molecular weight distribution commercial polymer, Styron.

Linear viscoelastic data were treated in an analogous manner. Isothermal data for the storage and loss moduli, G' and G'', were obtained and subjected to the usual temperature-frequency reduction (10)

$$G'_r = G' \frac{T_0}{T}, \qquad [8]$$

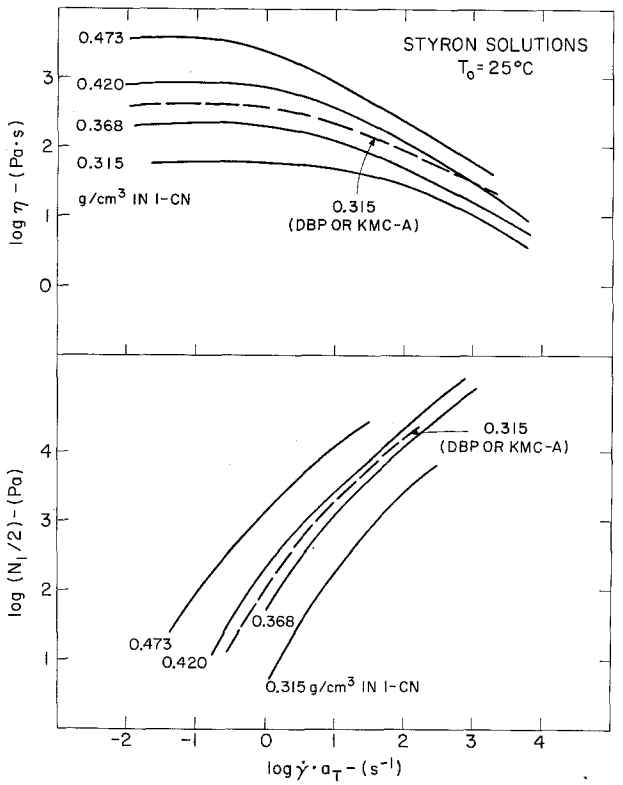

Fig. 6. Master curves for viscosity and the first normal-stress coefficient at 25 °C for broad molecular weight distribution polystyrene (STYRON) solutions. The concentrations and solvents are given for each curve

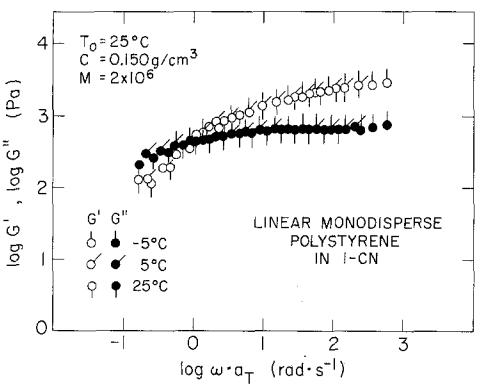

Fig. 7. Master curves for storage and loss moduli at 25 °C for the linear, monodisperse polystyrene solution in figure 1. The data from the three different temperatures shown were shifted using the same shift factors as for the viscosity

$$G_r'' = G'' \frac{T_0}{T}, \qquad [9]$$

$$\omega_r = \omega a_T. \qquad [10]$$

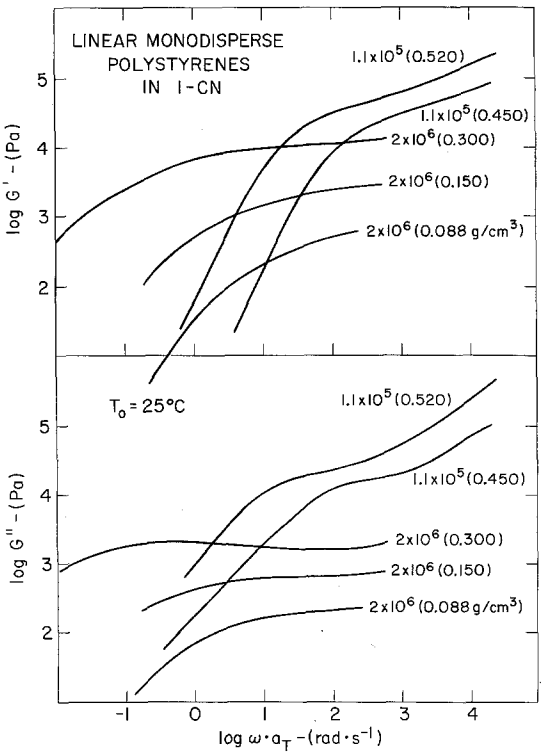

Fig. 8. Same as figure 4 but for the storage and loss moduli

An important feature of this temperature reduction is the fact that for each of the solutions listed in table 2, satisfactory reduction of the linear viscoelastic data was obtained using the same shift factors employed for reduction of the nonlinear steady shear flow material functions. An example of the linear viscoelastic master curves is shown in figure 7. Thus, we have observed that the activation energies obtained from the temperature dependence of the zero-shear-rate viscosity for each sample (fig. 2) and the a_T shift factors derived from these (eq. [4]) were suitable for describing the temperature dependence of all four material functions discussed in this paper. This temperature reduction scheme did not apply, however, to the viscometric data (18) obtained over the temperature range 160°C to 240°C for the undiluted Styron sample. For this polymer melt, the shift factors calculated from the temperature dependence of η_0 yielded successful reduction of the linear viscoelastic data; however, the viscosity data showed a systematic lack of superposition in the shear-rate-dependent region. Similar reduction anomalies for undiluted narrow molecular

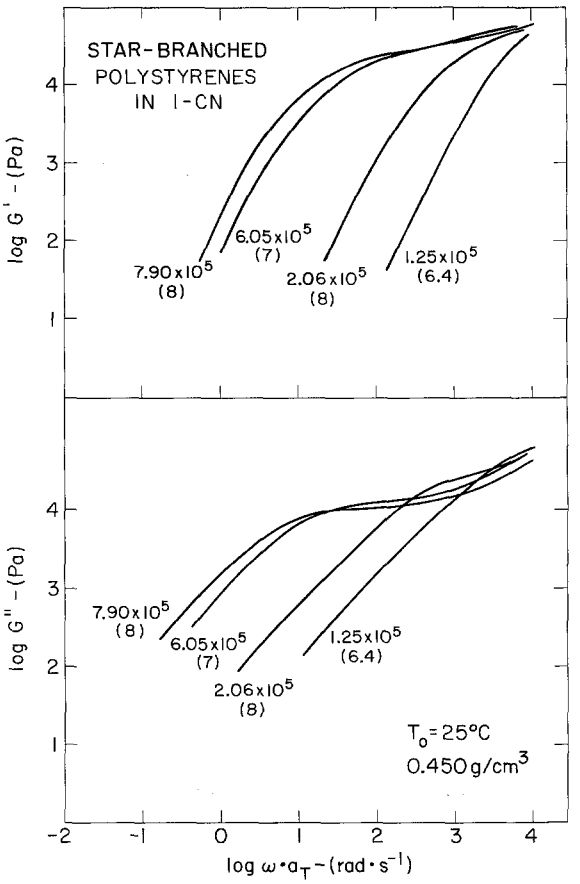

Fig. 9. Same as figure 5 but for the storage and loss moduli

weight distribution polystyrenes have been reported by Penwell et al. (2).

Figures 8 – 10 show linear viscoelastic master curves of the dynamic viscosity $\eta' \equiv G''/\omega$ and the storage modulus G'. These curves give the behavior of the same samples described in figures 4 – 6.

4. Discussion

From the results shown in the last section it is clear that with a cone-and-plate instrument it is possible to cover a much wider frequency range for $G^*(\eta^*)$ than can be covered in shear rate for the corresponding $\eta^\dagger$ properties. Here we have introduced a complex viscometric function $\eta^\dagger$:

$$\eta^\dagger(\dot{\gamma}) = \eta(\dot{\gamma}) - i\frac{1}{2}\dot{\gamma}\Psi_1(\dot{\gamma}) \qquad [11]$$

as a convenient short-hand notation.

Generally the frequency range we could cover was fixed at the lower end by transducer sensitivity and instrument noise and at the upper end by the largest rotation rate for the drive. For the viscometric properties we were similarly limited at low shear rates but we seldom could achieve the highest shear rates possible for the Mechanical Spectrometer because of the development of flow instabilities which we refer to as "shear fracture". Shear fracture is a failure in the sample parallel to the plates which begins at the free surface and then spreads inward toward the axis of rotation. The onset of shear fracture in our results is indicated by the maximum shear rate at which N_1 is given; η is reported to higher shear rates by virtue of the capillary experiments.

Hutton (9) has suggested that shear fracture will occur for sufficiently large values of the dimensionless group $N_1 R\theta_0/\sigma$ in which R is the plate radius, θ_0 is the cone angle and σ is the surface tension. It can be seen in figures 4 – 6 that shear fracture started when N_1 was approximately 10^4. For fixed $c\bar{M}_w$ this value is obtained at higher $\dot{\gamma}$ when c is low and $\bar{M}_w$ is high as is seen in figure 4; see also (18). As a result, previous studies have investigated the rheology of highly concentrated solutions by using low concentrations in combination with high molecular weights. This combination of c and $\bar{M}_w$ allows a more complete picture of the viscosity to be obtained (zero-shear-rate region through power-law region), but is does not faithfully model typical c and $\bar{M}_w$ values used industrially. In this investigation we wanted to study a wide range of $c\bar{M}_w$ behavior by varying both c and $\bar{M}_w$ separately; and in order to achieve the same wide shear rate range for viscosity as we obtained in frequency for η^* (particularly for high c and low $\bar{M}_w$) it was essential to have capillary viscometer results available. Unfortunately we could not obtain N_1 in the same manner, and thus we are not able to draw as many conclusions below about the elastic behavior of these polymer solutions as for the viscous behavior. Because of this limitation on easy measurement of $\eta^\dagger$ at large $\dot{\gamma}$ but not on η^* at large ω, it would clearly be useful to understand quantitatively under what conditions the linear data could be used to infer the viscometric data. More will be said about this below.

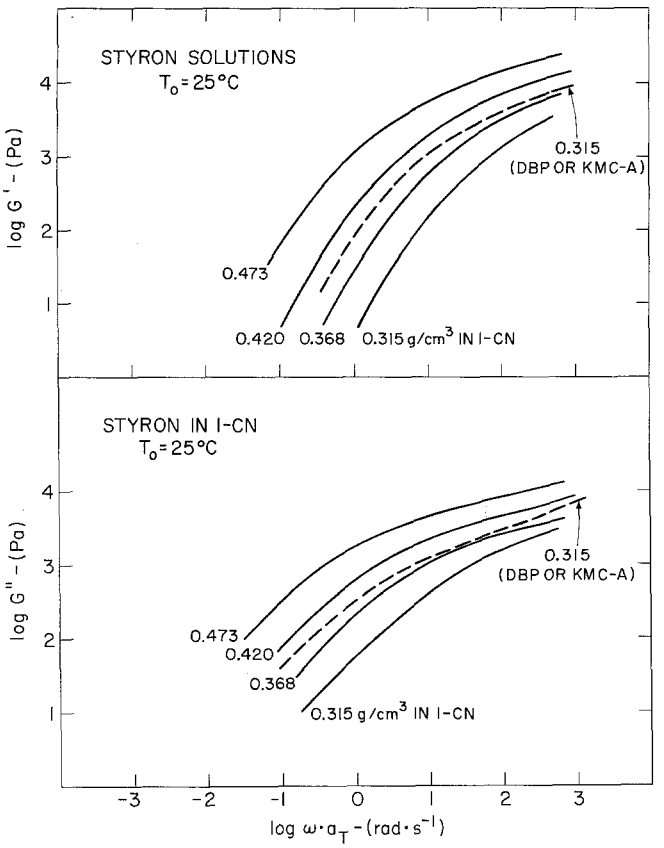

Fig. 10. Same as figure 6 but for the storage and loss moduli

Table 3. Modified Carreau equation parameters (see eq. [12])

Sample	η_0(Pa·s)	$\dot{\gamma}_0$(s^{-1})	ω_0(s^{-1})	λ(s)	λ'(s)	d	d'	a	a'
A1	73,000	$4.55 \cdot 10^{-2}$	$3.51 \cdot 10^{-2}$	22.0	28.5	0.861	1.075		
A2	1,400	$6.25 \cdot 10^{-1}$	$4.20 \cdot 10^{-1}$	1.60	2.38	0.800	0.997	1.25	1.25
A3	90	2.64	2.56	$3.79 \cdot 10^{-1}$	0.391	0.735	0.930	0.98	0.997
B1	8.080	$9.02 \cdot 10^{-1}$	$8.85 \cdot 10^{-1}$	1.109	1.13	0.696	1.018	2	1.91
B2	135	27.7	24.8	$3.61 \cdot 10^{-2}$	$4.03 \cdot 10^{-2}$	0.695	0.973	2	2
C1	1.180	10.8	10.6	$9.24 \cdot 10^{-2}$	$9.43 \cdot 10^{-2}$	0.559	0.826	2	2
C2	166	57.8	55.3	$1.73 \cdot 10^{-2}$	$1.81 \cdot 10^{-2}$	0.462	0.813	2	2.5
D1	3.930	10	7.04	10^{-1}	0.142	0.783	0.366	2	2
D2	15	$1.65 \cdot 10^{3}$	$2.22 \cdot 10^{3}$	$6.06 \cdot 10^{3}$	$4.50 \cdot 10^{-4}$			2	
E1	680	25.4	$1.98 \cdot 10^{2}$	$3.93 \cdot 10^{-2}$	$5.05 \cdot 10^{-3}$		0.279	2	
E2	4.03	$5 \cdot 10^{3}$		$2.0 \cdot 10^{-4}$		2			
F1	1,850	3.72	4.51	$2.69 \cdot 10^{-1}$	0.222	0.676	0.939	2	2.7
F2	33	97.1	$1.05 \cdot 10^{2}$	$1.03 \cdot 10^{-2}$	$9.52 \cdot 10^{-3}$	0.639	0.848	1.53	
G1	1,050	11.3	8.62	$8.86 \cdot 10^{-2}$	0.116	0.668	0.958	2	
H1	67	$1.15 \cdot 10^{2}$	$2.43 \cdot 10^{2}$	$8.70 \cdot 10^{-3}$	$4.27 \cdot 10^{-3}$	0.510	0.724	2	
J1	14	10^{3}	$2.06 \cdot 10^{3}$	10^{-3}	$4.85 \cdot 10^{-4}$	0.447	0.754	2	
K1	4089	1.0	0.752	1.0	1.329	0.614	0.75	1.21	0.90
K2	800	3.36	1.94	$2.98 \cdot 10^{-1}$	0.515	0.602	0.71	1.01	1.12
K3	200	10.4	7.30	$9.64 \cdot 10^{-2}$	0.137	0.586	0.137	1.23	1.14
K4	58	35.7	17.5	$2.80 \cdot 10^{-2}$	$5.73 \cdot 10^{-2}$	0.550	0.68	0.90	1.16
K5	2400	$6.41 \cdot 10^{-1}$		1.56		0.522	0.69		
K6	88	12.7		$7.85 \cdot 10^{-2}$		0.444			
K7	410	2.60	2.5	$3.84 \cdot 10^{-1}$	0.400	0.422	0.67	1.2	1.00
K8	375	2.07	3.15	$4.83 \cdot 10^{-1}$	0.317	0.352	0.70	2	1.16

Table 4. Zero-shear-rate and frequency elastic properties

Sample	$(2G'/\omega^2)_0$ (Pa · s^2)	J_e^R (from η^*, eq. [17])	$\Psi_{1,0}$ (Pa · s^2)	J_e^R (from $\eta^\dagger$, eq. [17])
A1			$5.0 \cdot 10^6$	$1.68 \cdot 10^{-1}$
A2			$7.0 \cdot 10^3$	$3.19 \cdot 10^{-1}$
A3	$1.32 \cdot 10^2$	$8.54 \cdot 10^{-1}$	$1.2 \cdot 10^2$	$7.77 \cdot 10^{-1}$
B1	$8.7 \cdot 10^3$	$1.83 \cdot 10^{-1}$	$9.2 \cdot 10^3$	$1.94 \cdot 10^{-1}$
B2	5.1	$2.57 \cdot 10^{-1}$	7.7	$3.87 \cdot 10^{-1}$
C1	$1.05 \cdot 10^2$	$4.25 \cdot 10^{-1}$	$1.1 \cdot 10^2$	$4.45 \cdot 10^{-1}$
C2	2.2	$3.89 \cdot 10^{-1}$	3.5	$6.19 \cdot 10^{-1}$
D1	$5 \cdot 10^2$	$6.46 \cdot 10^{-1}$	$3.5 \cdot 10^2$	$4.52 \cdot 10^{-1}$
D2	$7.5 \cdot 10^{-3}$	$4.83 \cdot 10^{-1}$	$7.5 \cdot 10^{-3}$	$4.83 \cdot 10^{-1}$
E1	10	$9.13 \cdot 10^{-1}$	25	$2.28 \cdot 10^0$
E2	$2.6 \cdot 10^{-3}$	$4.91 \cdot 10^0$	$2.0 \cdot 10^{-2}$	$3.77 \cdot 10^{+1}$
F1	$4.3 \cdot 10^2$	$3.89 \cdot 10^{-1}$	$6.3 \cdot 10^2$	$5.70 \cdot 10^{-1}$
F2	$4.6 \cdot 10^{-1}$	$8.73 \cdot 10^{-1}$	$4.2 \cdot 10^{-1}$	$7.97 \cdot 10^{-1}$
G1	$1.7 \cdot 10^2$	$5.42 \cdot 10^{-1}$	$2.2 \cdot 10^2$	$7.02 \cdot 10^{-1}$
H1	$2.4 \cdot 10^{-1}$	$5.02 \cdot 10^{-1}$	$3.4 \cdot 10^{-1}$	$7.11 \cdot 10^{-1}$
J1	$4.0 \cdot 10^{-3}$	$4.00 \cdot 10^{-1}$	$1.05 \cdot 10^{-2}$	$1.05 \cdot 10^0$
K1	10^4		$3.0 \cdot 10^4$	
K2	834	1.77	$8.9 \cdot 10^2$	1.88
K3	63.5	1.89	32.6	0.97
K4	6.5	1.97	4.3	1.30
K7	3.6	1.91	$3.8 \cdot 10^2$	2.30
K8	320	2.31	$2.9 \cdot 10^2$	2.10

4.1. Effect of polymer structure and concentration on linear viscoelastic and viscometric properties

In order to assess quantitatively the effects of concentration, molecular weight, molecular weight distribution, and star-branching on the rheological properties, we fit the viscosity to a modified Carreau viscosity equation (18):

$$\eta = \eta_0[1 + (\lambda\dot{\gamma})^a]^{-d/a}. \qquad [12]$$

The parameters which we fit were η_0, λ – a characteristic time for the fluid, d – the negative of the power-law slope, and a. The parameter a, which is taken to be 2 in the Carreau equation (19), adjusts the breadth of the transition region between the zero-shear-rate viscosity and the power-law regions. A similar equation was used to describe $\eta'(\omega)$ with the corresponding dynamic parameters denoted with primes.

In table 3 the parameters defined by eq. [12] and its dynamic viscosity analog are listed for the solutions tested. In these tables we also list a critical shear rate $\dot{\gamma}_0$ (or critical frequency ω_0) at which η begins to decrease with shear rate; its value is simply $1/\lambda$. We do not give similar tables for $2G'/\omega^2$ and Ψ_1 because we did not have enough data to justify fits to anything but their limiting values at zero frequency and shear rate, respectively; these are given as $(2G'/\omega^2)_0$ and $\Psi_{1,0}$ in table 4, columns 2 and 4, respectively.

We now discuss the effects of structure and concentration on η_0, $\dot{\gamma}_0$ and ω_0, d and d', and $(2G''/\omega^2)_0$ and $\Psi_{1,0}$.

4.1.1. Zero-shear-rate viscosity

At low $c\bar{M}_w$ the zero-shear-rate viscosity of a star polymer solution is lower than that of a linear polymer solution of the same $c\bar{M}_w$ because the radius of gyration of the star polymer is smaller. This can be allowed for by g in eq. [2]. Thus we found that the best correlation between c, $\bar{M}_w$, and η_0 is

$$\eta_0 = 0.85\, c K_1^c (g\bar{M}_w)^y \qquad [13]$$

where

$$K_1 = 6.31 \cdot 10^{11},$$

$$y = \begin{cases} 1.0 & cg\bar{M}_w < M_c \\ 3.4 & cg\bar{M}_w > M_c \end{cases}$$

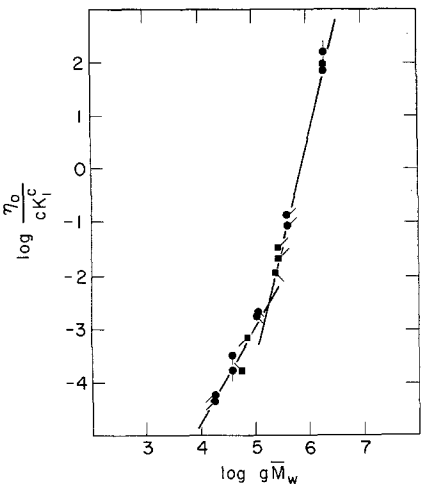

Fig. 11. Concentration and molecular weight dependence of the zero-shear-rate viscosity η_0 for monodisperse star and linear polystyrenes. The constant K_1 is equal to $6.31 \cdot 10^{11}$, and the factor g defined by eqs. [1] and [2] allows for size differences between star and linear polystyrenes of the same molecular weight at infinite dilution. Symbols are defined in table 2

in which M_c is the critical molecular weight for polymer-polymer interactions to affect η_0. In eq. [13], c and $\bar{M}_w$ are to have units g/cm^3 and g/mole, respectively in order to give the viscosity in Pa · s. Note that this correlation shown in figure 11 works equally well for both star-branched and linear polymers as long as $g\bar{M}_w$ is used in place of $\bar{M}_w$. We saw no "enhancement" of η_0 by the star-branched polymers for all our samples ($cg\bar{M}_w < 10^6$).

4.1.2. Critical shear rate and critical frequency

In order to examine the concentration and molecular weight dependence of $\dot{\gamma}_0$ and ω_0 we have used the following expression (18) for $\dot{\gamma}_0$ suggested by Graessley (10, p. 545; 20; 21)

$$\dot{\gamma}_0 = \frac{\pi^2 RT}{6}\left(\frac{c}{\eta_0 M} + \frac{c^2}{\rho_2 \eta_0 M_c}\right) \qquad [14]$$

in which ρ_2 is the solute density. A similar expression is given for ω_0. For low and high

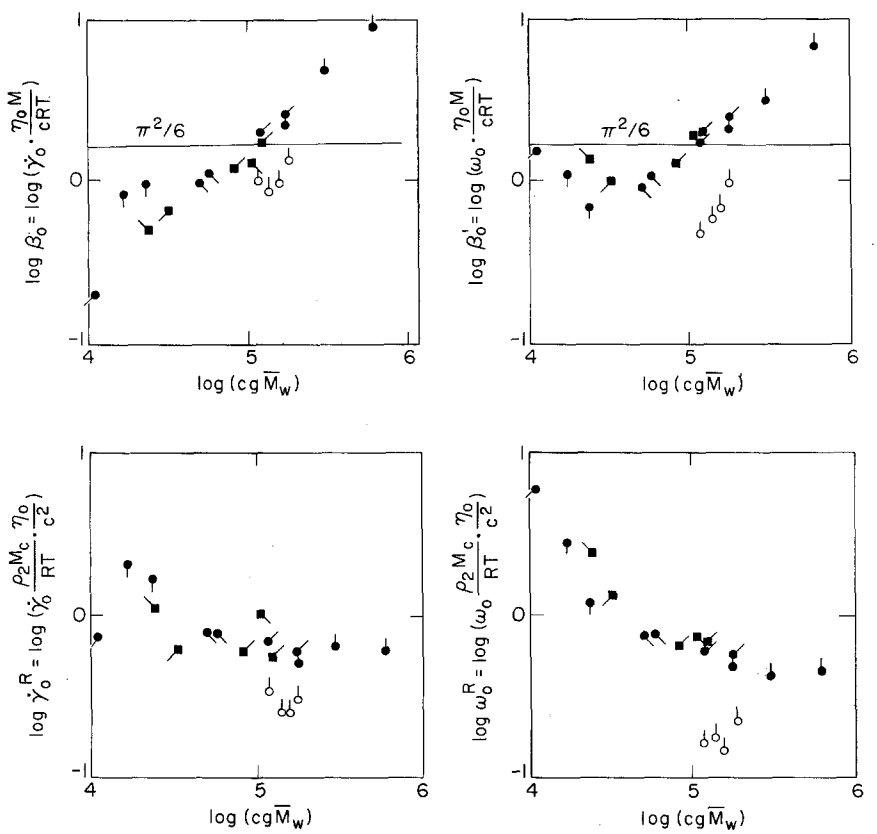

Fig. 12. Concentration and molecular weight dependence of the reduced critical shear rates and frequencies at which decreases from η_0 in η and η' are observed. Symbols are defined in table 2

concentrations the following dimensionless critical shear rates are obtained from eq. [14]:

$$c\bar{M}_w \ll \rho_2 M_c: \qquad \beta_0 \equiv \dot{\gamma}_0 \frac{\eta_0 M}{cRT}, \qquad [15]$$

$$c\bar{M}_w \gg \rho_2 M_c: \qquad \dot{\gamma}_0^R \equiv \dot{\gamma}_0 \frac{\rho_2 \eta_0 M_c}{c^2 RT}. \qquad [16]$$

Eq. [14] implies that both β_0 and $\dot{\gamma}_0^R$ should be equal to a constant, namely $\pi^2/6$ at low and high $c\bar{M}_w$, respectively. Identical definitions can be given for limiting values of reduced critical frequencies, β_0' and ω_0^R.

Figure 12 compares our results with Graessley's predictions. For polystyrene, $\rho_2 = 1.05$ and $M_c = 38{,}000$ (10, p. 409) so that $\log \rho_2 M_c$ is equal to 4.60. Though we do not have data for $\log c\bar{M}_w$ too much less than 4.6 it appears that β_0 and β_0' both approach constant limiting values at low $c\bar{M}_w$. Although there is a fair amount of scatter in the data, the constant value appears to be somewhat less than $\pi^2/6$. For $c\bar{M}_w \gg \rho_2 M_c$ both $\dot{\gamma}_0^R$ and ω_0^R are seen to approach constant values; again the prediction of $\pi^2/6$ overestimates the data.

For all of the narrow distribution polystyrene samples it is found that the critical shear rate $\dot{\gamma}_0$ and critical frequency ω_0 are the same. For the broad distribution polystyrene samples, on the other hand, we find that $\dot{\gamma}_0$ is greater than ω_0. It might be hoped that for the narrow distribution samples, since β_0 and β_0', and $\dot{\gamma}_0^R$ and ω_0^R successfully reduce different concentration and molecular weight data, that it might be possible to construct unified "master curves" for both $\eta(\dot{\gamma}, \bar{M}_w, c, T)$ and $\eta'(\omega, \bar{M}_w, c, T)$. This is not possible for these polystyrene samples primarily because the power-law slopes also depend on molecular weight and concentration.

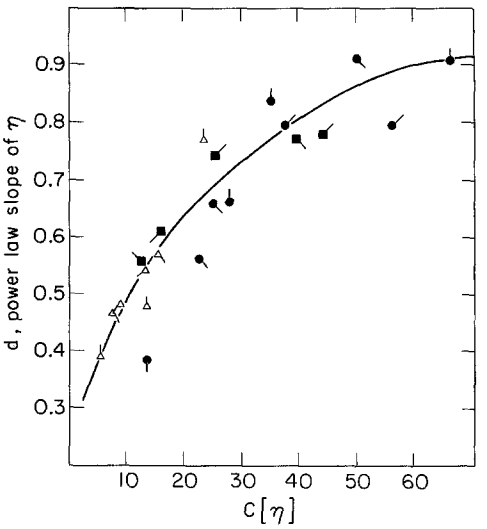

Fig. 13. Dependence of the power-law slope of viscosity on the product of concentration and zero-shear-rate intrinsic viscosity. Symbols are defined in table 2

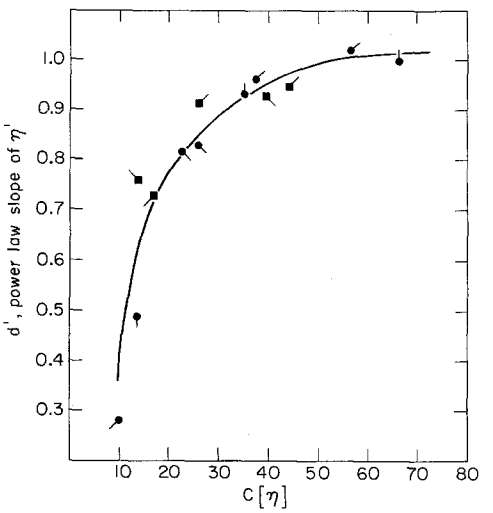

Fig. 14. Same as figure 13 but for the dynamic viscosity η'

4.1.3. Power-law slopes: d and d'

It is well-known that the power-law slopes for viscosity and dynamic viscosity, d and d', depend on concentration and molecular weight. It has furthermore been shown that d and d' can be correlated with the coil overlap parameter $c[\eta_0]$ (20, p. 132). In figures 13 and 14 we show d and d' as functions of $c[\eta_0]$. In figure 13 we have used Ashare's data (17) on narrow distribution polystyrene solutions in Aroclor to supplement the moderate $c[\eta_0]$ range. Although there is some scatter, the data are reasonably well correlated in this manner. No effect of star-branching is observed; it is not necessary to use g to correct for molecular size in this figure, as this correction is inherently contained in $[\eta_0]$. It is clear that though they have the same qualitative shapes, d and d' are different functions of $c[\eta_0]$. At large $c[\eta_0]$, d' is seen to exceed unity which, of course, is not physically possible for d. We are not sure if a limiting value for d had been reached at the highest values of $c[\eta_0]$ we were able to reach. It appears that d is still

increasing at $c[\eta_0] = 70$ and that its maximum value is in excess of 0.9.

4.1.4. Steady state compliance

We have already noted that our data do not allow conclusions to be drawn about the shear-rate dependence of Ψ_1. Since we have already given the effects of c and $\bar{M}_w$ on η_0, we describe structure and concentration effects on $\Psi_{1,0}$ by means of the steady state compliance J_e^0:

$$J_e^0 \equiv \frac{\Psi_{1,0}}{2\eta_0^2} = \lim_{\omega \to 0}\left(\frac{G'}{\omega^2\eta_0^2}\right). \quad [17]$$

It is not difficult to show from the Rouse model (22) that

$$J_e^0 = \frac{2}{5}\frac{M}{cRT}. \quad [18]$$

This suggests that a reduced steady-state compliance defined by

$$J_e^R = J_e^0 cRT/M \quad [19]$$

should be a constant, namely 2/5. A modification to the Rouse theory for star-branched polymers by Ham (11) gives

$$J_e^0 = \frac{2}{5} g_2 M/cRT \quad [20]$$

where g_2 is a size correction factor (different from g) given by

$$g_2 = \frac{15f - 14}{(3f - 2)^2}. \quad [21]$$

Thus if we define a reduced steady state compliance for stars as in eq. [19] except that g_2M replaces M, then we should get the same value as for the linear polystyrenes. Our data reduced in this way are given in table 4. In agreement with the above predictions we found no difference between J_e^R for narrow distribution star and linear polystyrenes. The values for J_e^R scattered about 0.4 for $c\bar{M}_w$ between 10^3 and 10^6. For the broad distribution samples, J_e^R was found to be slightly larger, about 1.0. It is significant that we see no enhancement in the size corrected J_e^R as a result of branching up to $c\bar{M}_w = 10^6$; similar findings were reported by Masuda et al. (14).

4.2. Similarities between η^* and η †

Figures 15–17 compare the shapes of the master curves for the viscometric and linear viscoelastic properties of typical linear, star-branched and broad molecular weight distribution polystyrene samples. In these figures direct comparisons can be made between the "viscous" material response $\eta'(\omega)$ and $\eta(\dot{\gamma})$ as well as the "elastic" parts G' and $N_1/2$. In addition we have included the magnitude of the complex viscosity which according to the well-

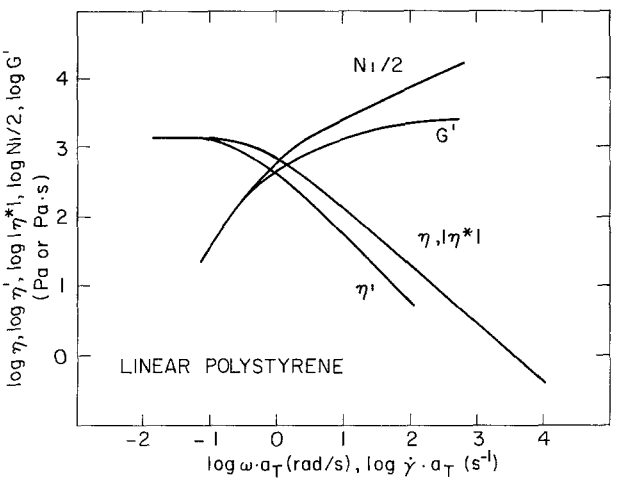

Fig. 15. Graphical comparisons between the viscous properties $\eta(\dot{\gamma})$ and $\eta'(\omega)$ and the elastic properties $N_1(\dot{\gamma})/2$ and $G'(\omega)$ for a linear, monodisperse polystyrene ($\bar{M}_w = 2 \cdot 10^6$) in 1-CN. Also shown is the magnitude of the complex viscosity $|\eta^*|$ which should equal η according to the Cox-Merz rule (eq. [22])

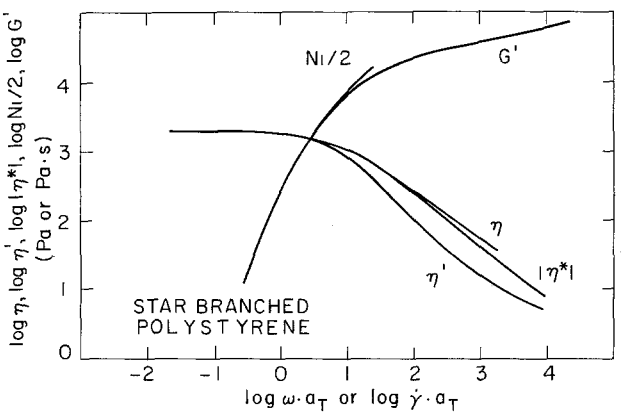

Fig. 16. Same as figure 15 but for a star-branched polystyrene solution (Sample F1)

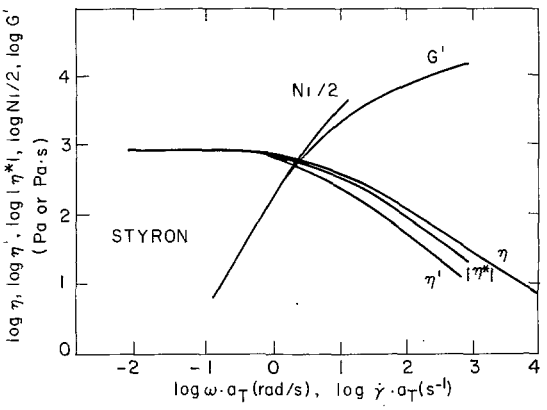

Fig. 17. Same as figure 15 but for a broad molecular weight distribution polystyrene solution (Sample K2)

known Cox-Merz rule (23) should numerically equal the viscosity when the shear rate and frequency are equal:

$$\eta(\dot{\gamma}) = |\eta^*(\omega)|_{\omega=\dot{\gamma}} = \sqrt{\eta'^2 + \eta''^2}\Big|_{\omega=\dot{\gamma}}. \quad [22]$$

Similar comparisons for all other samples we studied can be found elsewhere (18). Note that master curves obtained by time-temperature superposition can justifiably be used for these comparisons because we used the same shift factors a_T for both η^* and $\eta^\dagger$ data; as a result any conclusions reached from these master curves will not be temperature specific. In some previous studies different shift factors were used for linear viscoelastic and viscometric properties, so that any differences or similarities between the material functions may be functions of temperature.

In figure 15, the Cox-Merz rule is seen to describe accurately the data for a narrow distribution, linear polystyrene solution over the entire range of the two master curves. The dynamic viscosity is much smaller than the viscosity at high shear rates, and the storage modulus is much smaller than $(N_1/2)$ at high shear rates. In figure 16, the Cox-Merz rule is also seen to be in good agreement for a star-branched polystyrene solution except at high $\dot{\gamma}$ and ω. Again η' is well below η at high $\dot{\gamma}$ and ω. No corresponding statements about $(N_1/2)$ and G' are possible for this sample because the cone-and-plate flow became unstable before high shear rates were reached. Finally, figure 17 shows that for a broad distribution polystyrene solution, $\eta > |\eta^*| > \eta'$ at high shear rates/frequencies. At moderate $\dot{\gamma}$ and ω, $(N_1/2)$ is slightly larger than G'.

The findings on all other samples are summarized below. In every case the low shear-rate and low frequency properties showed the agreement that is expected for all rheologically simple fluids, namely,

$$\lim_{\dot{\gamma}\to 0} \eta(\dot{\gamma}) = \lim_{\omega\to 0} \eta'(\omega) = \eta_0, \quad [23]$$

$$\lim_{\dot{\gamma}\to 0} \Psi_1(\dot{\gamma}) = \lim_{\omega\to 0} \frac{2G'(\omega)}{\omega^2} = \Psi_{1,0}. \quad [24]$$

At moderate to high shear rates ($\dot{\gamma} \geqslant 1/\lambda$) most samples obeyed the Cox-Merz rule within experimental error. In this connection we note that had we used cone-and-plate data for this comparison we would have incorrectly concluded in many cases that $|\eta^*| > \eta$; more reliable data from the capillary viscometer gave $|\eta^*| = \eta$. The erroneously low viscosity from the cone-and-plate measurements at high shear rates is due to shear fracture.

Two types of exceptions to the Cox-Merz rule were observed at high shear rates:

1. $|\eta^*| > \eta > \eta'$. This was seen in sample A1 which is a high molecular weight, linear, narrow distribution polystyrene solution with $c\bar{M}_w = 6 \cdot 10^5$. Osaki et al. (5) found similar abnormalities in narrow distribution, linear polystyrene solutions in diethylphthalate when $c\bar{M}_w > 6.6 \cdot 10^5$.
2. $\eta > |\eta^*| > \eta'$. At the highest shear rates and frequencies we used, $|\eta^*|$ was 20 – 50% lower than η for all of the broad distribution polystyrene solutions. A similar deviation was found by Harris (20, 24) for a narrow distribution polystyrene solution in PCB with $c\bar{M}_w = 6 \cdot 10^4$ (high $\bar{M}_w$ and low c) and with high solvent viscosity. Within experimental error our data obtained on solutions of narrow molecular weight distribution polystyrenes did not show this deviation.

It is interesting that all solutions of star-branched polystyrene show good agreement with the Cox-Merz rule, although the viscometric properties of these solutions were difficult to obtain and show large amounts of scatter.

Because of shear fracture, the ranges of shear rates covered for N_1 were severely limited. Where we could obtain high shear rate data, $(N_1/2)$ was greater than G' for all samples. Because shear fracture will result in lower N_1 readings than the true values, the differences in $(N_1/2)$ and G' are probably even larger than we have shown in figures 15 – 17.

Outside of the low frequency regions for each of the samples ($\omega < 1/\lambda$) where eqs. [23] and [24] are known to hold, G' is much larger than G''. As a result the value of $|\eta^*|$ is dominated by the "elastic" contribution

$$|\eta^*| \approx \frac{G'}{\omega} \quad (\omega > \lambda^{-1}) . \qquad [25]$$

It seems very curious to us that in view of eq. [25] the Cox-Merz rule should be so successful. The implication is that the "elastic" response to a small amplitude shearing oscillation gives a good measure of the viscous response in high-shear-rate steady shear flow.

5. Conclusions

One of the principal results of this study is the acquisition of both linear viscoelastic and viscometric material functions on the same set of well-defined polymer solutions. Narrow-distribution linear and star-branched polystyrenes were used as well as broad-distribution commercial polystyrene. In addition a wide range of $c\bar{M}_w$ was covered by using both high concentrations with low molecular weight and vice versa.

The following effects of polymer structure, concentration, and molecular weight were observed for the rheological properties:

1. The zero-shear-rate viscosity for solutions of narrow distribution polystyrenes is given by

$$\frac{\eta_0}{0.085 c (6.31 \cdot 10^{11})^c} = \begin{cases} (g\bar{M}_w) & cg\bar{M}_w < M_c \\ (g\bar{M}_w)^{3.4} & cg\bar{M}_w > M_c \end{cases}.$$

The same relation applies equally to star branched as well as linear polystyrene as long as the size corrected molecular weight, $g\bar{M}_w$, is used as shown. This result is limited to $c\bar{M}_w < 6 \cdot 10^5$, which is the largest $c\bar{M}_w$ we studied (for linear polymers). For the star-branched polymers all our data is for $cg\bar{M}_w < 1.22 \cdot 10^5$. It is possible that above this value enhancement would be observed.

2. The critical frequency and shear rate were found to correlate with $c\bar{M}_w$ as suggested by Graessley.

3. The power-law slopes of η and η' correlated with $c[\eta_0]$. As $c[\eta_0]$ approaches 100, the power-law slope of η' exceeds unity whereas the power-law slope for η is between 0.9 and 1.0 but does not appear to have quite reached a limiting value. The correlations with $c[\eta_0]$ apply equally well to all of the narrow distribution samples, independent of structure.

4. The reduced steady-state compliance J_e^R (eq. [19]) is fairly constant over the range of conditions we studied and no enhancement is observed for the star-branched polystyrenes.

The Cox-Merz rule

$$\eta(\dot{\gamma}) = |\eta^*(\omega)|_{\omega=\dot{\gamma}}$$

was found to apply over a wide range of shear rates and frequencies for both linear and star-branched, narrow distribution polystyrene solutions. The exceptions to the application of this rule are

1. for $c\bar{M}_w > 5 \cdot 10^5$, $|\eta^*| > \eta$ at high $\dot{\gamma}$,
2. for broad molecular weight distribution polystyrenes, $\dot{\gamma}_0 > \omega_0$ and $\eta > |\eta^*|$ at large $\dot{\gamma}$.

Our data coupled with other data in the literature show then that unless $c\bar{M}_w$ is extremely high or the system is polydisperse, the Cox-Merz rule can be used up to high frequencies where the infinite frequency dynamic viscosity is approached.

There seem to be no close similarities between $N_1/2$ and G' outside of the zero-frequency/zero-shear-rate regions. We are unaware of a simple empiricism for relating these material functions which works as well as the Cox-Merz rule.

Acknowledgements

The authors wish to acknowledge the National Science Foundation for partial support of this work through the Research Initiation and Support (RIAS) program. One of the authors (K.Y.) gratefully acknowledges support from Oji Paper Co. during the course of this research. Finally, we wish to thank several groups for material and instrument assistance in this research: to Dr. P. Rempp of CNRS in Strasbourg for supplying us with the star-shaped polystyrenes, to Dr. J. Starita of Rheometrics Corp. for aid in acquiring forced oscillation cone-and-plate data, and to Dr. M. Hauber of Instron Corp. for aid in making low shear-rate measurements.

References

1) Isono, Y., T. Fujimoto, N. Takeno, H. Kajiura, M. Nagasawa, Macromolecules **11**, 888 (1978).
2) Penwell, R. C., W. W. Graessley, A. Kovacs, J. Polym. Sci., Physics **12**, 1771 (1974).
3) Raju, V. R., H. Rachapudy, W. W. Graessley, J. Polym. Sci., Physics **17**, 1223 (1979).
4) Onogi, S., H. Kato, S. Ueki, T. Ibaragi, J. Polym. Sci. **C15**, 481 (1966).
5) Osaki, K., M. Fukuda, S. Ohta, B. S. Kim, M. Kurata, J. Polym. Sci., Physics **13**, 1577 (1975).
6) Kajiura, H., Y. Ushiyama, T. Fujimoto, M. Nagasawa, Macromolecules **11**, 894 (1978).
7) Kotaka, T., M. Kurata, M. Tamura, Rheol. Acta **2**, 179 (1962).
8) Graessley, W. W., W. Park, R. Crawley, Rheol. Acta **16**, 291 (1977).
9) Hutton, J. F., Rheol. Acta **8**, 54 (1969).
10) Ferry, J. D., "Viscoelastic Properties of Polymers", 2nd ed., Wiley (New York 1970).
11) Ham, J. S., J. Chem. Phys. **26**, 625 (1957).
12) Graessley, W. W., T. Masuda, J. E. L. Roovers, N. Hadjichristidis, Macromolecules **9**, 127 (1976).
13) Leblanc, J. L., Rheol. Acta **15**, 654 (1976).
14) Masuda, T., Y. Ohta, S. Onogi, Macromolecules **4**, 763 (1971).
15) Noordermeer, J. W. M., O. Kramer, F. H. M. Nestler, J. L. Schrag, J. D. Ferry, Macromolecules **8**, 539 (1975).
16) Rochefort, W. E., G. G. Smith, H. Rachapudy, U. R. Raju, W. W. Graessley, J. Polymer Sci., Physics **17**, 1197 (1979).
17) Ashare, E., Trans. Soc. Rheol. **12**, 535 (1968).
18) Yasuda, K., Ph. D. Thesis, Massachusetts Institute of Technology, Cambridge, MA (1979).
19) Bird, R. B., R. C. Armstrong, O. Hassager, "Dynamics of Polymeric Liquids", Vol. 1, Wiley (New York 1977).
20) Graessley, W. W., Advances in Polymer Science, Vol. 16, "Entanglement Concept in Polymer Rheology" (1974).
21) Graessley, W. W., R. L. Hazelton, R. L. Lindeman, Trans. Soc. Rheol. **11**, 267 (1967).
22) Bird, R. B., O. Hassager, R. C. Armstrong, C. F. Curtiss, "Dynamics of Polymeric Liquids", Vol. 2, Wiley (New York 1977).
23) Cox, W. P., E. H. Merz, J. Polym. Sci. **28**, 619 (1958).
24) Harris, E. K., Jr., Ph. D. Thesis, University of Wisconsin, Madison, WI (1970).

Authors' addresses:

Dr. R. C. Armstrong, Dr. R. E. Cohen
Department of Chemical Engineering
Massachusetts Institute of Technology
Cambridge, MA 02139 (U.S.A.)

Dr. K. Yasuda
Oji Paper Co. Ltd.
Research Division, Tokyo Laboratory
1-10-6 Shinonome, Koto-Ku
Tokyo (Japan)